


AUTHOR QUERY FORM

	Journal: SE Article Number: 2981	Please e-mail or fax your responses and any corrections to: E-mail: corrections.essd@elsevier.sps.co.in Fax: +31 2048 52799
---	---	---

Dear Author,

Please check your proof carefully and mark all corrections at the appropriate place in the proof (e.g., by using on-screen annotation in the PDF file) or compile them in a separate list. Note: if you opt to annotate the file with software other than Adobe Reader then please also highlight the appropriate place in the PDF file. To ensure fast publication of your paper please return your corrections within 48 hours.

For correction or revision of any artwork, please consult <http://www.elsevier.com/artworkinstructions>.

Any queries or remarks that have arisen during the processing of your manuscript are listed below and highlighted by flags in the proof. Click on the 'Q' link to go to the location in the proof.

Location in article	Query / Remark: click on the Q link to go Please insert your reply or correction at the corresponding line in the proof
Q1	Please confirm that given names and surnames have been identified correctly.
Q2	Please check whether the typeset of equations are okay.
Q3	Please check the sentence 'A value of between...' for clarity, and correct if necessary.

Highlights

► Heat Flux Sensors have high error at low flux. ► A model is developed to compensate for this error in situ. ► It accounts for variations in operation conditions. ► Using the model RMSE decreased from more than 100 (W/m^2) to less than 10 (W/m^2). ► Calibration is done in situ without the need of lab equipment.



A model for improved solar irradiation measurement at low flux

Marwan M. Mokhtar*, Steven A. Meyers, Irene Rubalcaba, Matteo Chiesa*,
Peter R. Armstrong*

Laboratory for Energy and Nano-Science, Masdar Institute of Science and Technology, Abu Dhabi 54224, United Arab Emirates

Received 1 February 2011; received in revised form 10 December 2011; accepted 12 December 2011

Communicated by: Associate Editor Robert Pitz-Paal

Abstract

Accurate measurement of solar radiation heat flux is important in characterizing the performance of CSP plants. Thermopile type Heat Flux Sensors (HFSs) are usually used for this purpose. These sensors are typically reasonably accurate at high heat fluxes. However measurement accuracy drops significantly as the measured radiation is below 1 kW/m^2 , this often leads to underestimation of the actual flux. At the Masdar Institute Beam Down Solar Thermal Concentrator (BDSTC), measurement of fluxes ranging from 0 kW/m^2 to more than 100 kW/m^2 is required. To improve the accuracy of the sensors in the lower range around 1 kW/m^2 , we have performed a test under ambient (not-concentrated) sunlight. Such low irradiation levels are experienced in characterizing the concentration quality of individual heliostats. It was found during the test that the measurement at this low range is significantly affected by ambient conditions and transients in the HFS cooling water temperature. A Root Mean Square Error (RMSE) of more than 100 W/m^2 was observed even though we kept the transients in water temperature to a minimum. Hence we devised a model to account for this measurement error at this flux range. Using the proposed model decreased the RMSE to less than 10 W/m^2 . The application of the model on existing heat flux measurement installations is facilitated by the fact that it only employs easily measurable variables. This model was checked by using a test data set and the results were in good agreement with the training data set.

© 2011 Published by Elsevier Ltd.

Keywords: Heat Flux Sensor; Beam Down; Concentrated solar radiation; Flux gauge; Flux measurement

1. Introduction

Flux distribution measurement is an essential step in characterizing the optical performance of solar concentrating systems, especially during the receiver design phase. This paper addresses the uncertainty of solar irradiation measurement at low levels (around 1 kW/m^2) using Heat Flux Sensors (HFSs). Flux measurement in this range using HFS is often underestimated due to sensor losses to the environment. The experiments were conducted in the Beam Down Solar Thermal Concentrator (BDSTC) at the

Masdar Institute. The BDSTC is a point focus concentrator of around 280 m^2 of primary reflective area which comprises of 33 ganged-type heliostats with an 8.5 m^2 of reflective area consisting of 42 flat mirror facets.

Although the accuracy of HFS is acceptable near their full range, as the flux level drops the relative error in measurement increases to unacceptable level. Low flux levels are experienced when assessing the concentration quality and flux distribution of individual heliostats (Mokhtar, 2011; Mokhtar et al., 2010); hence, it was necessary to adapt the existing flux measurement system for measurement in this range.

The flux mapping system consists of a CCD camera affixed to the top of the tower in order to measure concentrated flux distribution on a white Lambertian ceramic tile surface $\sim 2 \text{ m}$ above ground level. Embedded within the

* Corresponding authors. Tel.: +971 2 810 9144; fax: +971 2 810 9901.

E-mail addresses: marwan.mukhtar@gmail.com (M.M. Mokhtar), mchiesa@masdar.ac.ae (M. Chiesa), parstrong@masdar.ac.ae (P.R. Armstrong).

Nomenclature

c_0, c_1, c_2, c_3	regression model coefficients	T_{SE}	sensing element temperature (K)
G_{HFS}	solar radiation measured by the HFS (W/m^2)	T_{sky}	effective sky temperature (K)
G_{IR}	net IR radiation measured by the PIR (W/m^2)	ΔT	temperature difference across the resistive wafer (K)
G_{PSP}	solar radiation measured by the PSP (W/m^2)	v	wind speed (m/s)
h_{cfv}	forced convection heat transfer coefficient ($W m^{-2} K^{-1}$)	V	voltage generated by the thermopile (mV)
h_{cn}	natural convection heat transfer coefficient ($W m^{-2} K^{-1}$)	$(\alpha AG)_{SE}$	effective absorptivity-area-incident radiation product of the sensing element (W)
$(h_c)_{SE}$	convection heat transfer coefficient from the sensing element ($W m^{-2} K^{-1}$)	ϵ_{SE}	emissivity of sensing element coating
$(h_r)_{SE}$	linearized radiation heat transfer coefficient from the sensing element ($W m^{-2} K^{-1}$)	δ	Seebeck coefficient (mV/K)
k	thermal conductivity of the resistive wafer material ($W m/K$)	σ	Stefan–Boltzmann constant ($W m^{-2} K^{-4}$)
\tilde{k}	dome heating correction factor	Abbreviations	
L	thickness of the resistive wafer (m)	BDSTC	Beam Down Solar Thermal Concentrator
n	number of hot (or cold) junctions of the thermocouple circuit	CCD	Charge Coupled Device
q_{net}	net heat flux across through the sensing element (W/m^2)	CSP	Concentrated Solar Power
T_a	ambient temperature (K)	GHI	Global Horizontal Irradiation
T_{case}	PIR case temperature (K)	HFS	Heat Flux Sensor
T_{dome}	PIR dome temperature (K)	PIR	Precision Infrared Radiometer
T_w	mean water temperature (K)	PSP	Precision Spectral Pyranometer
		RMSE	Root Mean Square Error
		SE	sensing element
		Wspd	wind speed

tiles at eight locations are HFS to measure the concentrated solar flux. HFSs are used to calibrate the images of the CCD camera to get an absolute flux map. However previous studies using similar CCD–HFS systems have highlighted several inaccuracies in using these HFSs for solar radiation measurement (Ballestrín et al., 2003, 2006; Kaluza and Neumann, 2001; Ulmer et al., 2004). A new method for flux mapping was recently proposed by researchers at Sandia National Labs (Ho et al., 2011) which eliminates the need for HFS; this method however requires the knowledge of the reflectivity map of the target (receiver).

In recent years, the National Institute of Standards and Technology has developed a standard method for calibrating Heat Flux Sensors (Tsai et al., 2004). A variable temperature blackbody (constructed from an electrically heated graphite tube) is used to maintain the radiation incident on the Heat Flux Sensor. Similar calibration techniques have been used by the Vatel Corporation (2001) which set the blackbody temperature at 1123 K, or at 2580 nm according to Wien's Displacement law. The spectral mismatch between these calibration methods and their use for solar radiation measurement has been noted to cause inaccuracies due to the varying spectral absorptive characteristics of the black surface (often Zynolyte) as a function of wavelength (Ballestrín et al., 2003; Kaluza and Neumann, 2001; Ulmer et al., 2004). Ballestrín et al.

(2003) compared HFS calibrated at a blackbody temperature of 850 °C, at Air Masses from 1 to 4 and with two different black coatings (Zynolyte and colloidal graphite) resulting in an average overestimation of 3.6% and 27.9% respectively. According to Ulmer et al. (2004) spectral differences can cause an even larger error when using a windowed HFS.

Based on the findings of the aforementioned studies, non-windowed sensors with Zynolyte coating are most suitable for solar applications, and thus were chosen for use in this study. Since the sensors are intended for solar radiation measurements, calibrations were performed under ambient solar radiation to decrease any spectral mismatch errors.

Although non-windowed sensors have a better spectral and angular response compared to their windowed counterparts, they suffer from an inherent problem; increased error due to variations in ambient conditions, where convection and radiation from the surface of the HFS will lead to underestimation of the actual flux. This is especially significant when the measured flux is low.

2. Preliminary testing of Heat Flux Sensors (HFSs)

In the BDSTC, concentrated solar radiation on the target is measured using eight HFS distributed around the central focal point. Depending on the location of the

HFS, solar irradiation and number of heliostats in focus the measured flux can vary from less than 1 kW/m^2 to more than 100 kW/m^2 . Hence the HFS's are required to be able to measure in that range, where the greatest inaccuracy is expected to be in the range $<1.0 \text{ kW/m}^2$.

Fig. 1 depicts the measurement of the HFS using simple linear model based on factory calibration. The figure shows that the uncorrected measurement of the HFS is not adequate at low fluxes; an RMSE of more than 100 W/m^2 was calculated. It can also be noticed from Fig. 1 that the percent error is highest at low flux, when the measured flux increases, the percent error in measurement decreases.

In the 1980s Mulholland et al. (1988), performed calibrations of similar sensors for solar applications, where they used polynomial fits for calibrating the sensors under realistic operation conditions. In this paper we present an *in situ* method for calibrating non-windowed HFS for the use in BDSTC flux measurement system, in contrast with (Mulholland et al., 1988) however, the calibration model we are suggesting is based on a physical heat transfer model which employs easily measurable variables and which can account for variations in ambient and operation conditions, this is in contrast with simplified linear or polynomial fits.

The reference instrument used in the experiments is an Eppley Precision Spectral Pyranometer (PSP) (Eppley-Laboratory, 2011). The PSP is connected to the data acquisition device (a Campbell Scientific CR1000) through a differential voltage measurement. Combining the sensitivity of the PSP and the measurement resolution of the CR1000 results in an overall resolution of 0.406 W/m^2 . The accuracy of the CR1000 is 0.2% of the reading (25 mV), since the sensitivity of the PSP is $121.80 \text{ W m}^{-2}/\text{mV}$, this results in an uncertainty of 6.09 W m^{-2} caused by the CR1000. The uncertainty of the PSP itself is 1% due to temperature dependence and 0.5% linearity errors. More details can be found in Campbell-Scientific (2001).

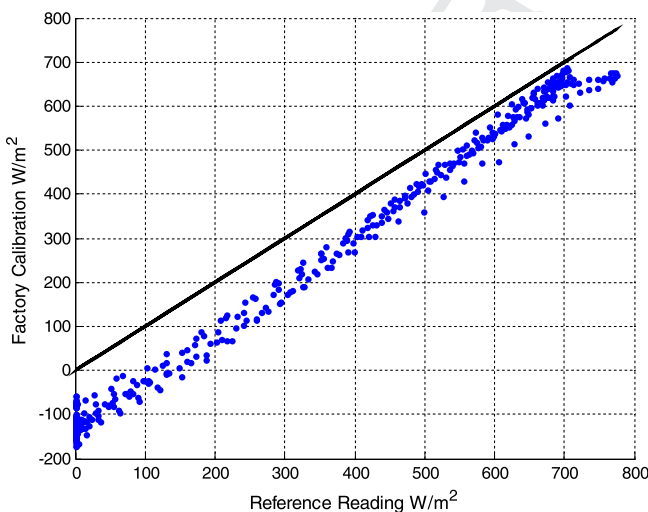


Fig. 1. Radiation flux using factory calibration versus the radiation flux measured by the reference instrument (RMSE = 115 W/m^2).

The HFS used is a Schmidt Boelter from Medtherm Corporation (Model No. 64-1SB-20, Serial No. 161544), with a full scale measurement of $1.0 \text{ BTU ft}^{-2} \text{ s}^{-1}$. The sensitivity of the HFS is $0.08130 \text{ BTU ft}^{-2} \text{ s}^{-1}/\text{mV}$ which is equivalent to $923.73 \text{ W m}^{-2}/\text{mV}$. The uncertainty specified by the manufacturer is 3.0% of its sensitivity. Our result shows that with a proper calibration model the instrument accuracy can be 3.0% of reading which is much better than 3.0% of full scale when measuring low flux!

3. Principle of operation of Heat Flux Sensors (HFSs)

A typical Schmidt-Boelter HFS is shown in Fig. 2. The Sensing Element (SE) consists of a thin thermally resistive layer (aluminum wafer in this case). A temperature gradient is established across this thin wafer where a net heat flux occurs.

According to Fourier's law of conduction and assuming a unidirectional axial conduction, this heat flux is related to the temperature gradient by:

$$q_{\text{net}} = -k \frac{dT}{dx} \quad (1)$$

A thermocouple across the resistive wafer measures the developed temperature gradient and thus the net heat transfer can be inferred using the finite form of Eq. (1) for a very thin wafer:

$$q_{\text{net}} \cong -k \frac{\Delta T}{L} \quad (2)$$

where ΔT is the temperature difference, L is the thickness of the resistive wafer and k is the thermal conductivity of the resistive wafer material.

The thermopile voltage output is given by the Seebeck relation, where n is the number of hot (or cold) junctions of the thermocouple circuit and δ is the Seebeck coefficient

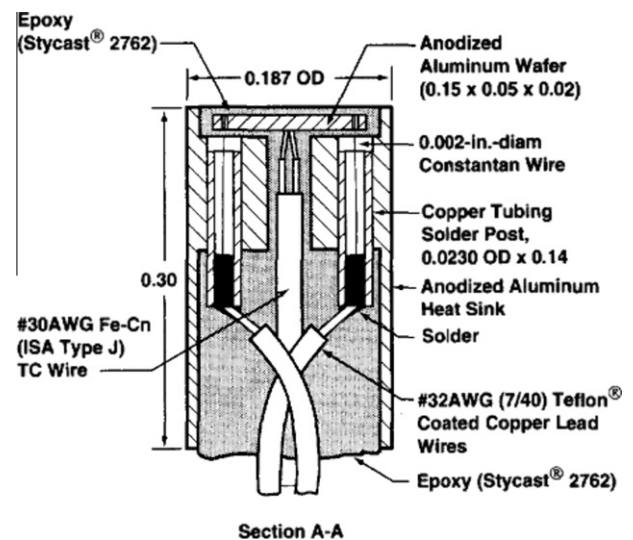


Fig. 2. Inner construction of a typical HFS (but not of the exact model used) (Kidd and Nelson, 1995).

(more details on this can be found in Kidd and Nelson (1995)):

$$V = \delta n \Delta T \quad (3)$$

Hence from Eqs. (2) and (3) we can write the sensitivity (S) of the HFS in mV/W as:

$$S = \frac{V}{q_{\text{net}}} = \delta n \frac{L}{k} \quad (4)$$

4. Heat transfer model

A simple energy balance on the sensing element shows that this measurement will be affected by convection and radiation in addition to conduction in the radial direction.

$$q_{\text{net}} = q_{\text{solar}} - q_{\text{convection}} - q_{\text{sky radiation}} - q_{\text{conduction_radiat}} \quad (5)$$

Since the thermopile is very thin, the radial conduction term can be neglected. However, convective and sky radiation terms can be quite significant and have to be considered for accurate measurement. Thus Eq. (5) can be expanded to give:

$$\frac{k}{\delta n L} V = \alpha_{\text{SE}} G - h_{\text{cn}}(T_{\text{SE}} - T_a) - \tilde{h}_{\text{cf}} v (T_{\text{SE}} - T_a) - \sigma \epsilon_{\text{SE}} (T_{\text{SE}}^4 - T_{\text{sky}}^4) \quad (6)$$

where α_{SE} is the absorptivity of the sensing element which is typically painted with a black coating, G is the incident solar radiation on the surface of the sensor in W/m^2 , h_{cn} is the natural convection heat transfer coefficient in $\text{W m}^{-2} \text{K}^{-1}$, $\tilde{h}_{\text{cf}} v$ is the forced convection heat transfer coefficient in $\text{W m}^{-2} \text{K}^{-1}$, v is local wind speed in m s^{-1} , σ is Stefan-Boltzmann constant in $\text{W m}^{-2} \text{K}^{-4}$ and ϵ_{SE} is the emissivity of sensing element. The temperatures are T_{SE} for the sensing element, T_a for ambient temperature, T_{sky} for effective sky temperature all in K. The calibration coefficient given by

the manufacturer in $\text{W m}^{-2}/\text{mV}$ includes the effect of the absorptivity along with the term $(\frac{k}{\delta n L})$, hence:

$$G_{\text{HFS}} = G - \frac{h_{\text{cn}}}{\alpha_{\text{SE}}} (T_{\text{SE}} - T_a) - \frac{\tilde{h}_{\text{cf}} v}{\alpha_{\text{SE}}} (T_{\text{SE}} - T_a) - \frac{\sigma \epsilon_{\text{SE}}}{\alpha_{\text{SE}}} (T_{\text{SE}}^4 - T_{\text{sky}}^4) \quad (7)$$

5. Experimental setup

The experimental setup in Fig. 3 consists of a thermopile type (Schmidt-Boelter) HFS with an open and flat receiving surface. Cooling water is supplied to the sensor from a well insulated tank with enough thermal mass to eliminate the transients in water temperature. The flow rate through the sensor is high and constant to ensure that the sensor body temperature is uniform. Inlet and outlet temperatures are monitored using T-Type thermocouples inserted inside the tubes using a T-joint pointing upstream to enhance heat transfer. The high flow rate keeps the average difference between the inlet and outlet below about 0.3 K.

The sensors are tested under ambient sunlight and solar irradiation (GHI) is measured by a ventilated Eppley Precision Spectral Pyranometer (PSP) (we use a reference sensor with the correct spectral response for calibration, rather than a reference source). In addition a Li-COR PV pyranometer is also used for comparison. A ventilated Precision Infrared Radiometer (PIR) is used to measure sky radiation; compensation is done using the temperature measurement of both the dome and the case to infer the sky temperature. The equation is provided by the manufacturer (Eppley Labs) and is shown here after rearranging and including dome heating correction. A value of between (3.5 and 4) is recommended by Albrecht and Cox (1977) as cited in Eppley-Laboratory (2006).

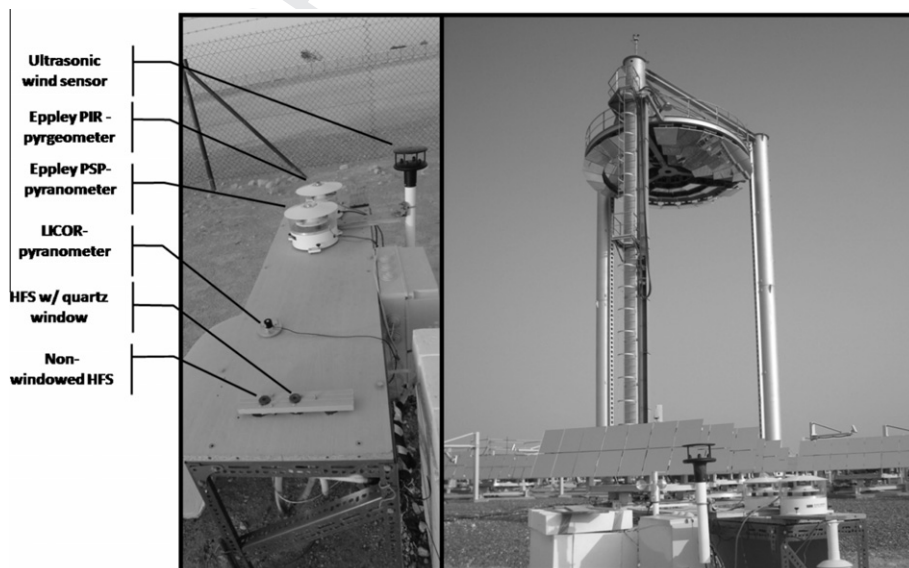


Fig. 3. Right: BDSTC tower and heliostat field with experimental setup in front, left: details of the experimental setup.

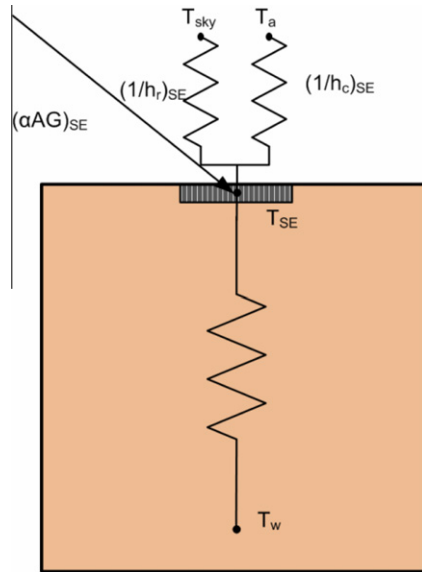


Fig. 4. Electrical analog for the HFS heat transfer model.

$$G_{IR} = -\sigma \epsilon (T_{case}^4 - T_{sky}^4) + \tilde{k} \sigma (T_{dome}^4 - T_{case}^4) \quad (8)$$

An ultrasonic 2D wind sensor measures wind speed and direction, unlike typical 3-cup anemometer this sensor does not have a measurement dead zone at the beginning of its range (the 3-cup can only measure starting from 0.4 m/s). In addition it has better resolution. Ambient temperature is measured using a shielded T-type thermocouple. The sampling rate of the whole acquisition system is 0.1 Hz.

6. Linear regression model

Fig. 4 shows an approximate electrical circuit analog used to model the HFS. The resistance between the mean

water temperature (T_w) and the sensing element temperature (T_{SE}) is an effective resistance for many conductive paths that depend on the construction of the sensor.

The temperatures T_{SE} and T_w shown in Fig. 4 vary almost in unison in the companion sensor which is equipped with body and sensor thermocouples (see Fig. 5). And we note that the variations in $T_{SE} - T_w$ (RMSE < 0.5 K) are much less than the variations in $T_{SE} - T_a$, based on this, in the proposed linear model of Eq. (9) we have replaced T_{SE} by T_w , this was done since T_w can always be measured whereas most sensors are not equipped with SE thermocouples.

Therefore we propose a regression model based on Eq. (7); with T_w substituted for T_{SE} as follows:

$$G_{PSP} = c_0 G_{HFS} + c_1 (T_w - T_a) + c_2 v (T_w - T_a) + c_3 (T_w^4 - T_{sky}^4) \quad (9)$$

The original data set used for regression consists of 16 days, with data sampled at 10-s intervals; the data set in use is reduced to only 10 days. The other 6 days were removed from the data set because they were cloudy/hazy days or due to measurement interruptions. The data set is further split into training and test data sets where every other day is taken for one set. Hence each set consists of 5 days. The test data set is used to assess the strength of the model predicted by the training data set. This is important to make sure that the model is not over fitting the data used to predict its parameters and therefore loses its generality.

Table 1 below shows the coefficients of the regression model of Eq. (9). As expected c_0 is very close to unity ($c_0 = 1.070$) which the physical model in Eq. (7) suggests. The increase from the ideal value of unity might be a result of degraded absorptivity of the SE coating (the sensor was

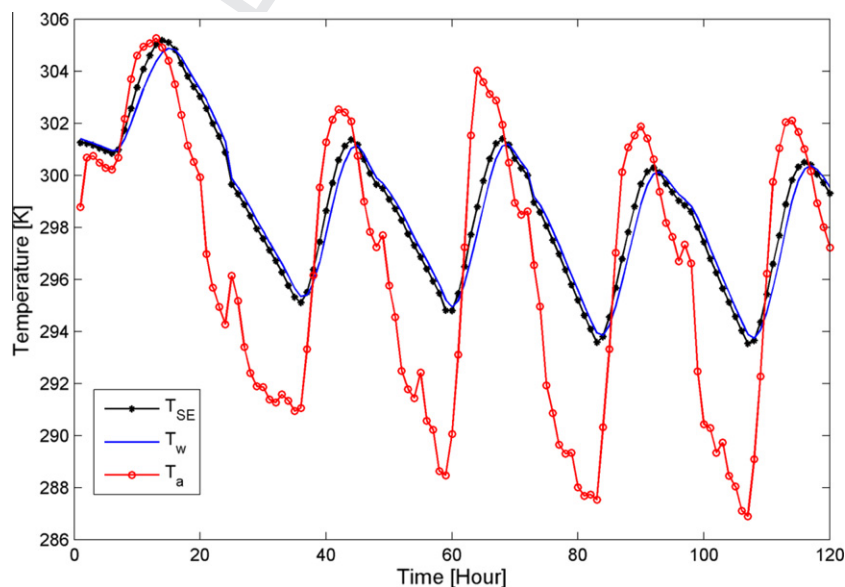


Fig. 5. Variation of sensing element temperature T_{SE} , mean water temperature T_w and ambient temperature T_a .

Table 1

Coefficients and statistics of the regression model of Eq. (9), RMSE = 6.31 W/m², R² = 99.94%.

Explanatory variable	Units	Coefficient	Confidence interval		t-Statistic
G_{HFS}	W/m ²	$c_0 = 1.070$	1.069	1.070	1153.400
$(T_m - T_2)$	K	$c_1 = 8.601$	8.573	8.629	152.000
$v(T_m - T_2)$	km/s	$c_2 = 3.138$	3.113	3.162	63.161
$T_m^4 - T_{sky}^4$	K ⁴	$c_3 = 5.666E-08$	5.661E-08	5.672E-08	503.850

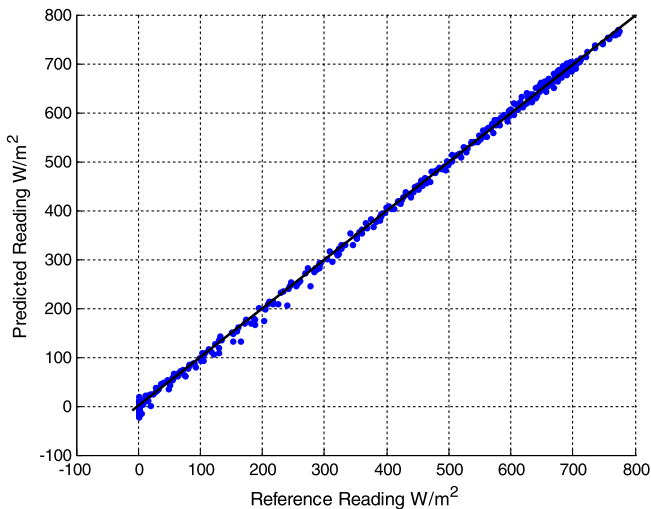


Fig. 6. Radiation flux predicted using the proposed model of Eq. (9) versus the radiation flux measured by the reference instrument (RMSE = 6.3 W/m²).

operation principles of the HFS. Moreover, the t -statistics of the coefficients and the confidence intervals support this opinion.

Fig. 6 shows the radiation flux predicted using the proposed model applied to the output of the HFS versus the radiation flux measured by the reference instrument (PSP).

We can see that the proposed model in Eq. (9) accurately represents the reading of the HFS with an RMSE of around 6.3 W/m² compared to RMSE of around 115 W/m² for the uncorrected reading, which is a significant improvement.

7. Residuals

We noticed some records with very high error in both the raw and the corrected readings of the HFS. The data shown is an average of 60 records which indicates that these errors are not a result of measurement noise but that of a phenomenon which lasts more than 10 min (60 samples). After investigating the setup, it was noticed that a nearby post (one of the BDSTC tower posts) was partially shading the test rig in the early mornings. This phenomenon is shown in Fig. 7. Data points that experienced this phenomenon (two points, i.e. 20 min data) were removed from the training data set and regression was run again. In addition, there was another extreme point removed, but the reason behind the high error was not determined.

Fig. 8 depicts the residuals of the model against the four explanatory variables. It can be seen from the figures that the errors are for the most part randomly distributed. A

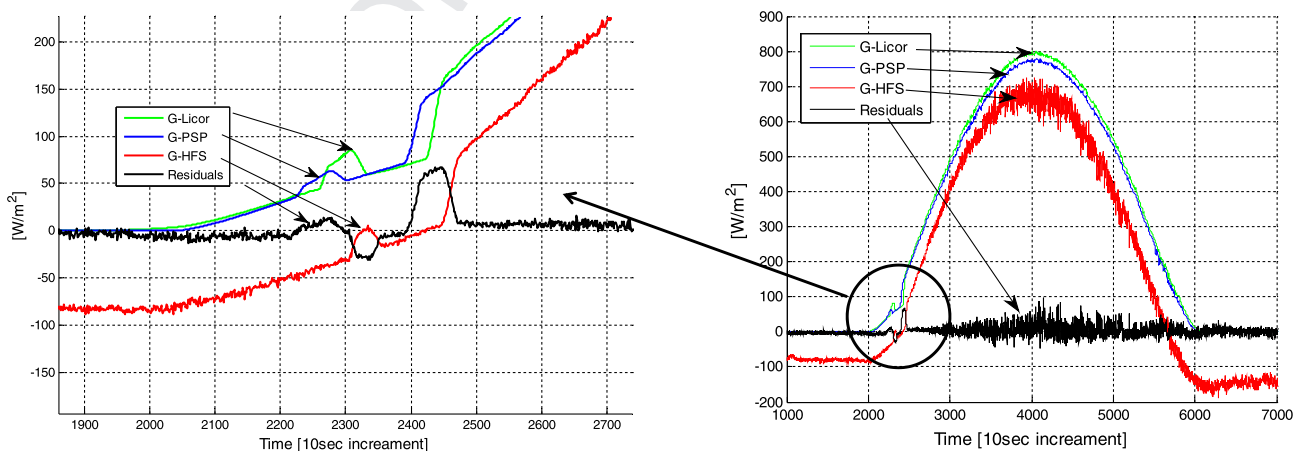


Fig. 7. Error due to shadowing of the test rig in early morning. On the left a zoomed-in view where one can observe how shadow is progressing, first shading the PSP then the Licor and last the HFS.

minor linear trend can be noticed when the residuals are plotted against the reference solar radiation, which might be a result of the **nonlinearity** of the HFS thermopile output and/or the conductivity of the SE material with temperature changes. However this trend can be neglected for the sake of a simplified model, a liner fit to the residuals gives a very small slope ($3.816\text{E}-4$).

Four points draw attention in Fig. 8. These points appear to be outliers and after investigation it was found

that these points are successive and belong to the morning of **1** day, we have not determined the reason that caused this error though.

To further test the model we applied it on a test data set of measurements which were taken on different days with similar conditions. The residuals distributions for the test data set are shown in Fig. 9. The RMSE of the test data set was found to be around 6.6 W/m^2 which is close to the original RMSE of the training data set of around 6.3 W/m^2 .

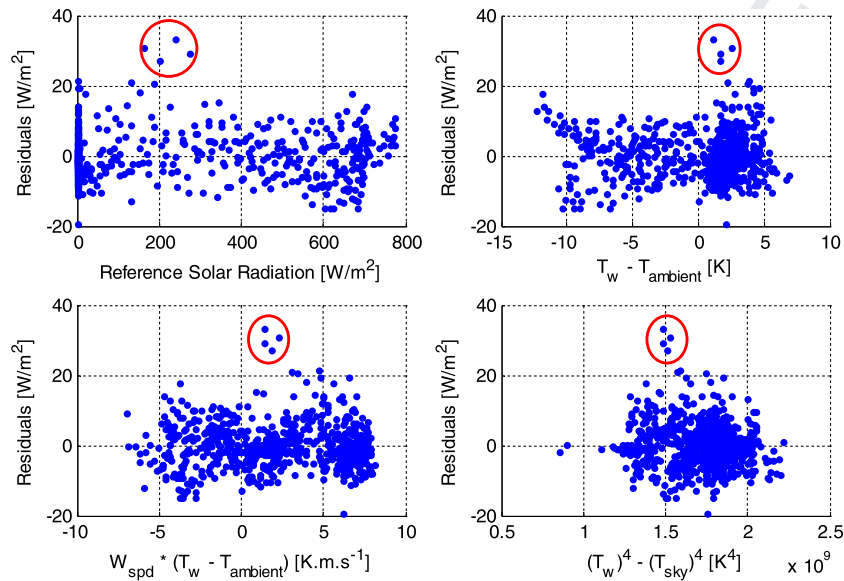


Fig. 8. Residuals distribution versus explanatory variables.

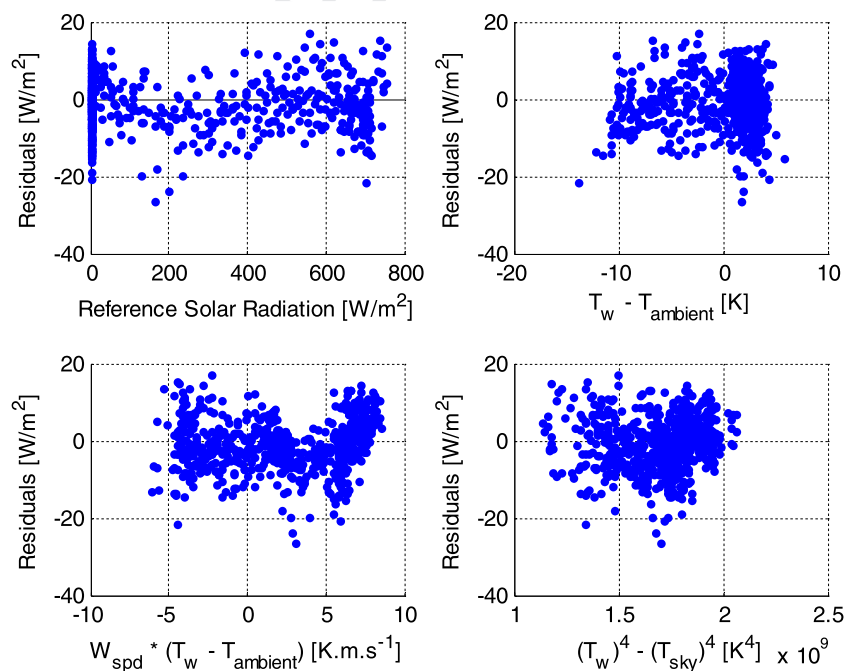


Fig. 9. Residuals distribution versus explanatory variables for the test data set.

8. Conclusion

The proposed model reduces the measurement error significantly, especially at low radiation fluxes. Using the sensor without correction will result in an underestimation of measured flux. An RMSE of more than 100 W/m^2 can be expected for uncorrected measurement of the HFS, however using the proposed model and by keeping the transients in cooling water temperature to a minimum, significantly higher measurement accuracy can be achieved, and RMSE of less than 10 W/m^2 can be obtained. This corresponds to an accuracy of around 3% of reading rather than 3% of full scale as specified by the manufacturer, which is a big improvement. Compared to simplified calibration models found in the literature, this model is expected to work on wider range of operating conditions since it models the source of errors individually rather than correcting for their collective effect. Moreover, since the model is based on easily measurable variables it can be applied conveniently on existing measurement systems without major modifications.

References

- Albrecht, B., Cox, S.K., 1977. Procedures for improving pyrgeometer performance. *J. Appl. Meteorol.* 16, 188–197.
- Ballestrín, J., Ulmer, S., Morales, A., Barnes, A., Langley, L.W., Rodríguez, M., 2003. Systematic error in the measurement of very high solar irradiance. *Solar Energy Mater. Solar Cell* 80, 375–381.
- Ballestrín, J., Estrada, C., Rodríguez-Alonso, M., Pérez-Rábago, C., Langley, L., Barnes, A., 2006. Heat flux sensors: calorimeters or radiometers? *Sol. Energy* 80, 1314–1320.
- Campbell-Scientific, 2001. Eppley PSP Precision Spectral Pyranometer Application Note. <<http://www.campbellsci.com/documents/technical-papers/epp-ppsp.pdf>> (accessed 10.12.11).
- Eppley-Laboratory, 2006. Precision Infrared Radiometer Instruction Sheet. The Eppley Laboratory.
- Eppley-Laboratory, 2011. Precision Spectral Pyranometer Specifications Sheet. <<http://www.eppleylab.com/PrdPrecSpectralPyrmttr.htm>> (accessed 10.12.11).
- Ho, C.K., Khalsa, S.S., Gill, D., Sims, C.A., 2011. Evaluation of a new tool for heliostat field flux mapping. In: Proceedings of 17th International Symposium on Concentrated Solar Power and Chemical Energy Technologies, 20–23 September 2011, Granada, Spain.
- Kaluza, J., Neumann, A., 2001. Comparative measurements of different solar flux gauge types. *J. Solar Energy Eng.* 123, 251–255.
- Kidd, C.T., Nelson, C.G., 1995. How the Schmidt-Boelter gage really works. In: Proceedings of the 41st International Instrumentation Symposium, 7–11 May 1995, Denver, CO, USA.
- Mokhtar, M., 2011. The Beam-Down Solar Thermal Concentrator: Experimental Characterization and Modeling. Master's Thesis. Masdar Institute of Science and Technology, Abu Dhabi, United Arab Emirates.
- Mokhtar, M., Rubalcaba, I., Meyers, S., Qadir, A., Armstrong, P., Chiesa, M., 2010. Heliostat field efficiency test of beam down CSP pilot plant experimental results. In: Proceedings of 16th International Symposium on Concentrated Solar Power and Chemical Energy Technologies, 21–24 September 2010, Perpignan, France.
- Mulholland, G., Hall, I., Edgar, R., Maxwell, C., 1988. Flux gage calibration for use in solar environments. *Sol. Energy* 41, 41–48.
- Tsai, B.K., Gibson, C.E., Murthy, A.V., Early, E.A., Dewitt, D.P., Saunders, R.D., 2004. Heat-Flux Sensor Calibration. National Institute of Standards and Technology Report, pp. 250–265.
- Ulmer, S., Lüpfer, E., Pfänder, M., Buck, R., 2004. Calibration corrections of solar tower flux density measurements. *Energy* 29, 925–933.
- Vatell-Corporation, 2001. Update on Heat Flux Calibration Standard Improvements. Heat Flux Newsletter. <<http://www.vatell.com/newsletterapril01.pdf>> (accessed 10.12.11).